Middle Pleistocene lower back and pelvis from an aged human individual from the Sima de los Huesos site, Spain

Alejandro Bonmatí[a,b], Asier Gómez-Olivencia[a,c], Juan-Luis Arsuaga[a,b,1], José Miguel Carretero[d], Ana Gracia[a,e], Ignacio Martínez[e,a], Carlos Lorenzo[f,a], José María Bérmudez de Castro[g], and Eudald Carbonell[f]

[a]Centro Mixto Universidad Complutense de Madrid–Instituto de Salud Carlos III de Evolución y Comportamiento Humanos, 28029 Madrid, Spain; [b]Departamento de Paleontología, Facultad de Ciencias Geológicas, Universidad Complutense de Madrid, 28040 Madrid, Spain; [c]Leverhulme Centre for Human Evolutionary Studies, University of Cambridge, Cambridge CB2 1QH, United Kingdom; [d]Departamento de Ciencias Históricas y Geografía, Facultad de Humanidades y Educación, Universidad de Burgos, 09001 Burgos, Spain; [e]Área de Paleontología, Departamento de Geología, Universidad de Alcalá de Henares, 28871 Alcalá de Henares, Spain; [f]Institut de Paleoecologia Humana i Evolució Social, Área de Prehistoria, Universitat Rovira i Virgili, 43005 Tarragona, Spain; and [g]Centro Nacional de Investigación sobre la Evolución Humana, 09004 Burgos, Spain

Contributed by Juan-Luis Arsuaga, August 31, 2010 (sent for review May 14, 2010)

We report a nearly complete lumbar spine from the Middle Pleistocene site of the Sima de los Huesos (SH) that is assigned to the previously published SH male Pelvis 1 [Arsuaga JL, et al. (1999). *Nature* 399: 255–258]. The "SH Pelvis 1 individual" is a unique nearly complete lumbo-pelvic complex from the human Middle Pleistocene fossil record, and offers a rare glimpse into the anatomy and past lifeways of *Homo heidelbergensis*. A revised reconstruction of Pelvis 1, together with the current fossil evidence, confirms our previous hypothesis that the morphology of this pelvis represents the primitive pattern within the genus *Homo*. Here we argue that this primitive pattern is also characterized by sexual dimorphism in the pelvic canal shape, implying complicated deliveries. In addition, this individual shows signs of lumbar kyphotic deformity, spondylolisthesis, and Baastrup disease. This suite of lesions would have postural consequences and was most likely painful. As a result, the individual's daily physical activities would have been restricted to some extent. Reexamination of the age-at-death agrees with this individual being over 45 y old, relying on the modern human pattern of changes of the articular surfaces of the os coxae. The presence of degenerative pathological lesions and the advanced age-at-death of this individual make it the most ancient postcranial evidence of an aged individual in the human fossil record. Additional nonpathological SH lumbo-pelvic remains are consistent with previous hypotheses, suggesting a less-pronounced sagittal spinal curvature in Neandertals compared with *Homo sapiens*.

human evolution | Sierra de Atapuerca | spino-pelvic morphology | paleopathology

Present knowledge of the evolution of the pelvic region and especially of the lower back in the human lineage is limited. Regarding the record of the genus *Homo*, the oldest evidence with associated lower back and pelvic remains is the *Homo ergaster* Nariokotome skeleton (KNM-WT 15000) from the Lower Pleistocene. However, this skeleton's juvenile developmental stage, pathological condition (1), and incomplete nature complicate an understanding of its fully adult morphology. Several Upper Pleistocene Neandertal skeletons preserve significant portions of these regions (Kebara 2, Shanidar 1 and 3, La Chapelle-aux-Saints, Régourdou 1, and La Ferrassie 1 and 2, among others). The pelvic morphology of *Homo neanderthalensis* differs from that of modern *Homo sapiens*. Neandertals exhibit pronounced lateral iliac flaring (resulting in a transversely wide pelvis), robust acetabulo-cristal buttress, well-developed supraacetabular sulcus and anterior superior iliac spine, and long and craniocaudally flattened superior pubic ramus (2–4). Based on the kyphotic lumbar vertebral bodies, some scholars propose the existence of a natural kyphosis in Neandertals (5), but others characterize their lumbar region as hypolordotic (6). Additionally, the Neandertal lumbar spine presents parasagittally oriented upper articular facets, long and laterally (in cranial view) and craniolaterally (in dorsal view) oriented transverse processes on the second and third lumbar vertebrae (L2, L3), and longer and more angled laminae in the fifth lumbar vertebra (L5) (7) that result in dorsoventrally elongated vertebral foramina (8). The available Plio-Pleistocene fossil record demonstrates that the character states of most of the Neandertal pelvic features are either primitive for the hominin clade or within the genus *Homo* (9–12). However, much more limited conclusions have been reached in the interpretation of the Neandertal lumbar vertebral morphology and lumbo-pelvic curvature.

We present a unique nearly complete Middle Pleistocene lumbo-pelvic complex from a single individual from the site of the Sima de los Huesos (SH) (Fig. 1). This individual, together with other specimens recovered from the SH site, elucidates the evolution of some major aspects of this region in our genus, especially concerning the emergence of Neandertal features. We also discuss the severe pathological lesions found in this individual that likely would have limited its range of physical activities to some extent. This individual represents the oldest postcranial evidence of an aged human in the fossil record.

Fossil Evidence

Since 1976, the SH site (Sierra de Atapuerca, Spain) has yielded more than 6,000 human remains attributed to *H. heidelbergensis*. In our view, this is an exclusively European species and is ancestral only to Neandertals (13, 14). This fossil collection has been dated to a minimum age of 530 kiloyears (kyr) (15). A minimum of 28 individuals of both sexes and diverse ages-at-death has been identified based on the dental evidence (16). In the 1994 field season, a nearly complete pelvis (Pelvis 1) was recovered and attributed to a large male older than 35 y old (11), which could correspond to one of the oldest (>35 y old) dental individuals from the site [i.e., Individual V, XIII, or XXI (16)]. To date, the sample of pelvic remains (os coxae and sacrum) is composed of 152 fragments [minimum number of elements (MNE) = 39; minimum number of individuals (MNI) = 16] (17). In addition, 435 vertebral fragments have been recovered from the site (MNE = 203; MNI = 13) (8). From this sample, it has been possible to reliably associate five lumbar vertebrae (L1–L5) with Pelvis 1 (Fig. 1). The inventory, labeling, and description of the pelvic and lumbar remains of the SH Pelvis 1 individual, and the criteria for their determination and association can be found in *Materials and Methods* and *SI Appendix*

Author contributions: A.B., A.G.-O., J.-L.A., J.M.C., A.G., I.M., and C.L. designed research; A.B., A.G.-O., J.-L.A., J.M.C., A.G., I.M., C.L., J.M.B.d.C., and E.C. performed research; A.B., A.G.-O., J.-L.A., and J.M.C. contributed new reagents/analytic tools; A.B., A.G.-O., J.-L.A., J.M.C., A.G., I.M., and C.L. analyzed data; and A.B., A.G.-O., J.-L.A., J.M.C., and A.G. wrote the paper.

The authors declare no conflict of interest.

[1]To whom correspondence should be addressed. E-mail: jlarsuaga@isciii.es.

This article contains supporting information online at www.pnas.org/lookup/suppl/doi:10.1073/pnas.1012131107/-/DCSupplemental.

Fig. 1. To date, the SH Pelvis 1 individual is composed of the nearly complete pelvis and lumbar spine.

(Texts S1, S2, and Table S1). In parallel, a new reconstruction of Pelvis 1 has also been completed.

Results

Pelvis 1: A Revised Reconstruction. The first reconstruction of Pelvis 1 (11) suffered from some asymmetries, mainly concerning the nonmidsagittal position of the pubic symphysis and the asymmetrical orientation of both ossa coxae relative to the sacrum. An attempt was made to reconstruct Pelvis 1 from scratch, aiming to minimize these asymmetries yet still preserve the overall anatomical consistency (see *Materials and Methods* and *SI Appendix*, Text S3). The general appearance and pelvimetry of the first and the revised reconstructions are noticeably similar. Although the pelvic rim of the new reconstruction shows reduced asymmetries, the position of both ossa coxae is still not completely symmetrical with respect to the midsagittal axis (*SI Appendix*, Fig. S1 and Table S2). We conclude that the actual pelvic rim morphology of this individual exhibits some degree of in vivo asymmetries, probably related to several anomalies detected in the sacrum (see below). In any case, SH Pelvis 1 is generally consistent with the pelvic anatomy observed in other SH remains attributed to this anatomical region.

SH Pelvis 1 Individual Updated. ***Developmental stage and age-at-death.*** Numerous pelvic remains from SH preserve, entirely or to some extent, the sacro-iliac joint, the pubic symphysis, and the acetabulum. The set of these articular surfaces signify different stages of remodeling, as has been described for modern humans (see *SI Appendix*, Table S3 for references). Based on the modern human pattern and timing of remodeling for these surfaces, SH Pelvis 1 would belong to one of the oldest (if not the oldest) individuals of the SH pelvic fossil sample, with an age-at-death older than 45 y (*SI Appendix*, Fig. S2 and Table S3). This estimation is consistent with our previous assessment [>35 y (11)].

Stature, body mass, and encephalization quotient. Currently, there are three complete femora recovered from SH (Femur X, XII, and XIII; MNI = 2) that could be associated with SH Pelvis 1 (*SI Appendix*, Text S4). From the lengths of these three femora and the bi-iliac breadth of the recent SH Pelvis 1 reconstruction, the average stature and body mass ranges were estimated at 168.9 to 171.2 cm and 90.3 to 92.5 kg, respectively. These values are lower than our previous estimations [173.3–179.5 cm and 93.1–95.4 kg (11)] but markedly above the value obtained by Ruff (78.1 kg), who adjusts the SH Pelvis 1 bi-iliac breadth for greater pelvic ellipticity relative to modern humans (18). To estimate the encephalization quotient, we have used the upper- and lowermost values of the body mass range and the smallest and largest cranial capacities for the SH sample (19). The updated encephalization quotient range (3.1–4.0) is only slightly higher (+0.1–0.2) than the original estimate [3.0–3.8 (11)].

Intrapopulation variation and sex attribution. The morphological features establishing the male condition of the SH Pelvis 1 individual were not modified in the revised reconstruction (11) (*SI Appendix*, Fig. S3). In contrast, two new SH pelvic remains (an isolated pubic body, AT-3814+AT-3817+AT-3497, and a fairly complete os coxae, Coxal III) show the modern female-like morphology previously described in ref. 11: smaller size and lower robusticity, presence of moderate subpubic concavity, mediolaterally (M-L) larger pubic body, acute medial aspect of the lower pubic ramus, development of the ventral rampart, and wider subpubic angle and greater sciatic notch. However, the degree of dimorphism in these traits in the SH sample is not as great as that between the distinctive modern human male and female morphologies (see also ref. 20).

SH Pelvis 1 Individual Within Human Evolution. ***The pelvis.*** The suite of morphometric features characterizing the first description of Pelvis 1 and the SH sample (11) remains valid for the recent reconstruction and for more recently recovered SH pelvic remains (*SI Appendix*, Table S4). The morphological pattern seen in the SH sample is largely shared by *H. ergaster*, Middle Pleistocene humans, and Neandertals, suggesting that this is the primitive condition within the genus *Homo* from which modern humans departed (11) (Fig. 2). Within this primitive pattern, Neandertals are distinguished by an extreme craniocaudal thinning of the superior pubic ramus, contrasting with the thick and robust modern human pubic ramus. Regarding this trait, the SH sample (n = 12; MNI = 7) is of intermediate thickness between *H. neanderthalensis* and *H. sapiens* (11) (*SI Appendix*, Table S5). An intermediate thickness of the pubic ramus is also present in the late Middle Pleistocene *Homo* specimen from Jinniushan (10), and this may represent the condition from which the Neandertal and *H. sapiens* morphologies diverged.

The pelvic canal shape can be quantified using the indices between the sagittal and transverse diameters at the inlet, midplane, and outlet planes. The evolution of the canal shape within the genus *Homo* is a matter of debate because of the limited and fragmentary fossil evidence. Modern humans show larger transverse (M-L) than sagittal (anteroposterior, A-P) dimensions in the inlet (inlet index < 100%; M-L oval shape) but larger A-P than M-L dimensions in the midplane (midplane index > 100%; A-P oval shape) (*SI Appendix*, Fig. S4). The outlet shows great

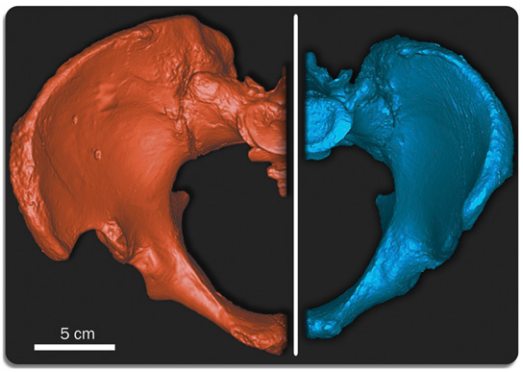

Fig. 2. Surface renderings showing the SH Pelvis 1 (*Left*, surface scan) vs. an anatomically modern male (*Right*, CT scan) of similar articular size in superior view, demonstrating the primitive (*Left*) vs. derived (*Right*) pelvic morphology within the genus *Homo*. SH Pelvis 1 vs. moden male dimensions: vertical acetabular diameter, 58.8 mm vs. 57.0 mm; maximum transversal sacral plate diameter, 52.3 mm vs. 51.5 mm; sagittal sacral plate diameter, 31.4 mm vs. 33.9 mm. Alignment of both elements was done using an 8 landmark registration algorithm in Mimics 13.0 (Materialise).

ANTHROPOLOGY

Table 1. Sagittal spino-pelvic morphometry in the SH sample and in Neandertals

	Sex	SAO	Z-score	PI	Z-score	Vertebral wedging† L1	Z-score	L2	Z-score	L3	Z-score	L4	Z-score	L5	Z-score
SH sample															
Pelvis 1 individual	♂	(70.60/75.52)‡	2.22*/2.74**	(23.78/27.63)‡	−2.64**/−1.98*			(4.56)	3.61**/3.76**	(4.53)	3.62**/4.32**	(3.71)	3.33**/3.79**	−1.06	1.54/1.75
Pelvis 2	♂			32.85	−1.91/−1.57										
VL10(L1)	♂					1.57	−0.71/0.46								
VL18(L2)	♀?							2.93	2.21*						
VL4(L4) + VL13(L5)	♀?											0.93	2.79**	−3.21	1.06
Neandertals															
Kebara 2	♂					2.78	0.45/1.48	3.39	2.51*/2.66**	3.62	2.91**/3.61**	1.54	1.97*/2.01*	−4.34	−0.89/−0.34
La Chapelle-aux-Saints	♂					3.92	1.55/2.45*							−3.31	−0.31/−0.13
Shanidar 3	♂					4.49	2.10*/2.93**	3.92	3.07**/3.09**	1.90	1.56/2.23*	0.08	0.74/1.12	−4.20	−0.79/−0.25

Raw values in sexagesimal degrees. Estimations in parentheses. See text for abbreviations. See *SI Appendix*, Texts S6 and S7, Fig. S6, and Tables S1 and S8 for material and method information. Z-score column represents the Z-score value (or range) for each fossil specimen calculated from the sex-corresponding Hamman-Todd (European and African American) and European (Spaniards) modern samples. Z-score = (Fossil value − Modern mean)/Modern SD. *, $P < 0.05$; **, $P < 0.01$.

†Positive and negative values indicate ventral (kyphotic vertebral bodies) and dorsal (lordotic vertebral bodies) wedging, respectively.

‡Values correspond from left to right to (*i*) nonreconstruction and (*ii*) reconstruction of the sacral promontory.

shape variability but, on average, it is the most rounded of the three pelvic planes (*SI Appendix*, Fig. S4) (*contra* ref. 21; see *SI Appendix*, Text S5). Regarding the sexually dimorphic pattern, females have significantly lower indices than males only in the midplane and outlet (*t* test; $P < 0.0001$ and $P < 0.001$, respectively), but not the inlet (*t* test; $P = 0.461$).

Regarding the shape of the pelvic canal of the fossils considered to represent the primitive *Homo* pattern (*SI Appendix*, Fig. S5), the two female archaic pelves from Gona (BSN49/P27) (12) and Tabun Cave (Tabun C1) (21) and the male SH Pelvis 1 show a M-L oval shape characterizing the inlet and outlet (inlet and outlet indices < 100%) (see also *SI Appendix*, Text S5 for comments on other reconstructions of these and other pelvic remains). The midplane has an A-P oval shape in SH Pelvis 1 (midplane index = 112.7%), but a nearly round shape in the Gona specimen [midplane index = 97.3% (12)]. Furthermore, the values of the indices of the two archaic female pelves (Tabun and Gona) are remarkably lower than those of the male SH Pelvis 1 in the pelvic midplane and outlet, but not in the inlet.

Comparison of the modern and fossil pelvic canal shape (*SI Appendix*, Text S5 and Fig. S5) reveals that: (*i*) A significantly more platypelloid midplane was present in the archaic *Homo* specimens than in modern humans. The midplane indices in the male SH Pelvis 1 and the female Gona pelvis fall at or below 2 SD from the male and females means of the modern sample, respectively. Concerning the inlet and outlet of Pelvis 1, Gona, and Tabun C1, only the remarkably low outlet index of the last is significantly different from modern humans (< 2 SD). (*ii*) The differences between the fossil male (SH Pelvis 1) and female (Gona and Tabun C1) *Homo* specimens can be attributed to sexual dimorphism in the pelvic canal. These archaic *Homo* pelves parallel the modern sexually dimorphic pattern (i.e., females showing remarkably lower indices than males in the midplane and outlet).

The lumbar vertebrae. The overall size (maximum dorsoventral diameter) of the most complete lumbar vertebrae (L3–L5) of this specimen is similar to the mean (L4) or significantly larger (L3 and L5) than our modern male comparative samples, and close to or slightly larger than those Neandertal males preserving the lumbar region (7, 22, 23) (*SI Appendix*, Tables S4 and S6). The transverse processes in L3 and L5 are significantly longer than modern human males and similar (L5) or even longer (L3) than in Neandertals. The orientation of the transverse process (i.e., the horizontal angle) of the L3 in the SH Pelvis 1 individual is dorsolateral in cranial view and lateral in dorsal view, similar to that in modern humans and Lower Plesitocene *Homo*. In contrast, the L3 in Neandertals show more laterally oriented transverse processes in cranial view and more cranially oriented processes in dorsal view (7). Finally, the SH Pelvis 1 individual and another L5 from SH (VL12) show neither the long and markedly sagittally oriented laminae nor the dorsoventrally enlarged canal described in Neandertals (7). Thus, the orientation (but not the length) of the transverse processes of the L3 and the sagittal orientation of the laminae that result in a large canal in L5, are derived Neandertal features not present in the Middle Pleistocene sample from SH ($n = 2$).

Sagittal Lumbo-Pelvic Morphology. The sacral anatomical orientation (SAO), the pelvic incidence (PI), and the lumbar vertebral wedging have been measured in the SH Pelvis 1 individual (24–26) (*SI Appendix*, Text S6 and Fig. S6). These three variables are angular position-independent anatomical parameters. In modern humans, the SAO has been found to be strongly and negatively correlated with the PI ($r = -0.824$) (26). Modern humans also show significantly positive correlations between the pelvic anatomical parameter PI and the positional parameter sacral slope (SS) ($r = 0.63$–0.86) that in turn is also significantly positively correlated with the positional parameter lumbar lordosis (LL) ($r = 0.68$–0.89). These correlations between pelvic anatomical and spinal positional parameters apply to both normal (healthy) individuals and patients suffering from spondylolisthesis or degenerative disc diseases (27–30). Large values of PI are related to more vertically oriented sacral plates, the joint surface of the body

of the first sacral vertebra (S1), and accentuated LL. Thus, the normal sagittal spino-pelvic alignment in modern humans is the result of a combination between the interdependent anatomical and positional lumbo-pelvic parameters (see ref. 29 and references therein).

Compared with modern male samples, the SH Pelvis 1 individual's sacral plate is extremely horizontally oriented (very high SAO and very low PI values), and the L2–L4 vertebral bodies are exceedingly kyphotic (vertebral wedging > 0°) (Table 1 and *SI Appendix*, Table S7). The nonpathological Pelvis 2 from SH shows a PI value similar to Pelvis 1, and also well below the modern human sample means (Table 1 and *SI Appendix*, Table S7). Neandertals and other nonpathological vertebrae (an L2 and an L4) from SH also differ markedly from the modern human means for lumbar wedging but are not as extreme as the SH Pelvis 1 individual (Table 1 and *SI Appendix*, Table S7). Taken together, these anatomical parameters reveal that nonpathological SH specimens and Neandertals possess a reduced LL compared with modern humans (Fig. 3 *A* and *B*). However, the sagittal lumbo-pelvic morphology of the SH Pelvis 1 individual was affected by several pathologies (Fig. 3*C*).

Anomalies and Pathological Lesions of the SH Pelvis 1 Individual.

Description. L1–L4 vertebral segment. The L2 to L4 vertebral bodies show extreme wedging and bone remodeling of the ventral surface (Fig. 4 and *SI Appendix*, Fig. S7*A*). In addition, the L4 spinous process is remodeled: it exhibits an asymmetrical triangular shape with a larger right side and a blunted and irregular base, both in posterior and cross section areas.

L5 vertebra. The L5 shows bone remodeling with extensive new periosteal bone formation on the ventral surface of the body (Fig. 4 and *SI Appendix*, Fig. S7*B*). The spinous process is deviated to the right side relative to the midsagittal plane and is not fused to the left lamina. The spinous process also exhibits extensive remodeling that results in a blunted and irregular cranial surface. The left lower articular process shows extensive bone growth and is located more dorsally than its counterpart on the right side. The left pedicle shows an additional small extra-articular surface on its caudal aspect. The caudal end-plate shows a very large (30.5 × 8.0 × 7.4 mm) osteolytic lesion that runs parallel and close to the ventral edge of the body. The cancellous bone around the osteolytic lesion is more compacted. The vertebral body height is larger on its left lateralmost side (26.1 vs. 23.8 mm). Finally, the caudal end-plate shows pathological erosion on its ventral edge.

Sacrum. The anterior half of the sacral plate presents an anomalous convex and blunted shape ["dome-shaped" sacrum (30)] (Fig. 4 and *SI Appendix*, Fig. S8). An osteophytic aureole can be appreciated on the preserved portions of the ventral and lateral outer edges of the articular plate. The anterior portion of this aureole overflows inferiorly the outer ventral edge of the sacral plate, in a step-like shape. The left articular process displays extensive bone remodeling, extending to the sacral ala and showing a general coronal orientation with ventral migration of its cranial border. This facet is much larger and very irregular in shape when compared with its counterpart on the right side and with other nonpathological sacra from SH. Finally, the two auricular surfaces of the Pelvis 1 show a very different shape and size: although the left auricula reaches to the level of the superior margin of the third sacral foramina, the right one barely aligns with the inferior edge of the second one. However, none of these joints shows signs of bone remodeling or anomalous growth.

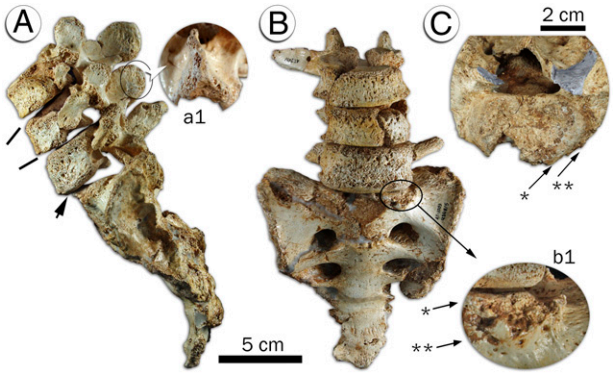

Fig. 4. L3–L5 segment and sacrum from the SH Pelvis 1 individual. (*A*) Left lateral view, depicting the extreme ventral wedging of the L4 (solid lines), the slippage of the L5 over the sacrum (lower arrow), and the remodelling of the caudal aspect of the L4 spinous process (a1). (*B*) Ventral view. Note the periosteal reactive bone in the ventral surface of the L5 body and the osteophytic rim (b1). (*C*) Detail of the S1 body in superior view, showing the differences between the superior articular processes (in gray). Note the ventral (b1) and lateral (*C*) separation between the margin of the sacral plate (*) and the osteophytic rim (**). No compensation has been made for the intervertebral discs.

The articulated pelvis. The sacral plate shows a lateral tilting to the left when the biacetabular axis is placed in a horizontal position (*SI Appendix*, Fig. S9).

Diagnosis and possible etiological factors. Developmental defects. The presence of the spinous process right of the midsagittal plane in the L5 and its nonunion to the left lamina are preliminarily attributed to a developmental hypoplastic defect of the left side of the neural arch. The position of this defect within the vertebral column (L5) and the absence of an enlarged neural canal rules out a neural tube defect of the developing spinal cord and thus of spina bifida cystica (31). However, the nonunion of the lamina could still be the product of a stress fracture or a trauma.

The normal appearance of the sacral auricular surface suggests that the asymmetry in these joints occurred before or during the period of the ossification of the sacro-iliac plate epiphyses [16–30 y of age in modern humans (32)] and well before the death of the SH Pelvis 1 individual. However, this asymmetry remains idiopathic.

Spondylolisthesis. The intense remodeling affecting the left articular processes between L5 and S1 could have led to the subluxation of the former over the latter, known as spondylolisthesis (33) (Figs. 3*C* and 4). This slippage might have involved a clockwise rotational component caused by the unilateral remodeling of the left side. This diagnosis is in agreement with the periosteal reactive bone on the anterior part of the L5 (34), the dome-shape of the sacral plate, and the distinctive osteophytic aureole of the S1 body and would be classified as spondylolisthesis "without separate arch" (35). The presence of a certain degree of asymmetry between the articular processes of the L5–S1 joint in the same vicinity as the asymmetrical sacral auricular joints and the neural arch defect in L5 suggest all these anomalies are likely developmental in origin. The nonparallel alignment between the biacetabular axis and the sacral plate would have created an instability that could have: exacerbated the asymmetry in the articular processes through bone remodeling and produced a scoliosis consistent with the asymmetry found in the lateral heights of the vertebral body of the L5.

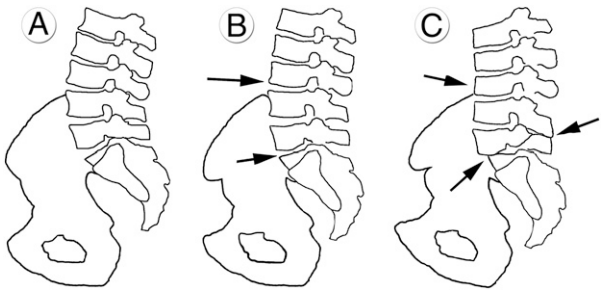

Fig. 3. A schematic view of the sagittal lumbo-pelvic configurations proposed in this study in standing position: (*A*) modern *H. sapiens*. (*B*) Neandertal lineage [kyphotic vertebral bodies in L1-L4 (hypolordotic spine) (upper arrow); more horizontally oriented sacral plate (lower arrow)]. (*C*) The SH Pelvis 1 individual reconstructed with the greatest degree of compensatory pelvic backtilt (horizontal sacral plate) [arrows from *Top* to *Bottom*: extremely kyphotic vertebral bodies (L2–L4); Baastrup disease (L4–L5); spondylolisthesis (L5–S1)].

The very large lytic lesion on the caudal L5 end-plate was previously diagnosed as a Schmörl's node, because of protrusion of the nucleus pulposus of the intervertebral disc into the vertebral body, followed by a reaction in the area affected (33). The herniation of the nucleus could have occurred when some degree of slippage of L5 over S1 had taken place and the position of the promontorium of the sacrum was approximately below the L5 lytic lesion. Additionally, the very dense cancellous bone around the lytic lesion could be the result of a reaction to the nucleus protrusion and to an infection.

Lumbar kyphotic deformity. The vertebrae of the SH Pelvis 1 individual have suffered a dramatic reduction of the ventral craniocaudal diameter of the vertebral bodies compared with nonpathological SH vertebrae (Figs. 3*C* and 4). This process has resulted in extremely kyphotic vertebral bodies in L2–L4 segment, and in slightly less lordotic body in L5 when compared with other SH individuals. These changes in their shape have been long and gradual and accompanied by the remodeling of the ventral surface of the vertebral bodies. The additional articular facet on the caudal aspect of the L5 demonstrates the loss of intervertebral space between the L5 and the sacrum because of disc degeneration.

The deformation of the vertebral bodies and the degeneration of the discs (at least at the L5–S1 level) in the SH Pelvis 1 individual would have further reduced the already attenuated LL characteristic of the healthy normal SH population (see above). This deformity may even have led to the inversion, from lordotic to kyphotic curvature, of the lumbar region of the SH Pelvis 1 individual, and it is likely to be of degenerative origin. Vertebral column deformities in modern humans that result in a kyphosis or a marked loss of lordosis in the lower back caused by degenerative changes are collectively termed lumbar degenerative kyphosis (36, 37). However, the dense cancellous bone around the L5 lytic lesion leaves open the possibility that this deformity could be also related to an infectious disease (e.g., tuberculosis).

The shape and degeneration of the spinous processes of L4 and L5 of the SH Pelvis 1 individual would be the result of their proximity and articulation termed Baastrup disease (38). In this individual, the spondylolisthesis between L5 and the sacrum, and the loss of disc space throughout the lumbar spine, must have been instrumental in the approximation of the spinous processes of L4 and L5.

Discussion

Evolutionary Context of the SH Spino-Pelvic Morphology. The sexual dimorphism in the modern human pelvic canal is the result of locomotor selective pressures for a narrow pelvis in both sexes combined with obstetrical selective pressures favoring wider canals at the midplane and outlet in females. Three archaic fossil pelves assigned to the genus *Homo* show a similar pattern of sexual dimorphism, suggesting similar obstetrical selective pressures were operating in the past and, at a minimum, can be taken as a sign of tight deliveries.

Regarding the lumbar curvature, nonpathological pelvic and lumbar specimens from the SH site and Neandertal individuals are consistent with the suggestion that the hypolordotic lumbar column in Neandertals (6) was already present in their Middle Pleistocene ancestors (Fig. 3*B*). Furthermore, significant positive correlations have been found between thoracic kyphosis and LL in modern humans (29). If these same correlations apply to the Neandertals and SH populations, it could be inferred that thoracic kyphosis in the Neandertal lineage was also attenuated compared with modern humans (*SI Appendix*, Fig. S10).

The sacra from SH ($n = 4$) show a dorsal rotation of the S1 body relative to the body of the second vertebra (S2) (*SI Appendix*, Text S2 and Fig. S8*B*). This dorsal rotation was termed a "second promontory" in the Kebara 2 Neandertal (22) and is also present in the Neandertal sacrum from Subalyuk. In modern humans, the PI is strongly correlated with the shape of the sacrum: the highest PI values are found when the S1 sacral plate and the S2 caudal plate converge anteriorly (27). The relationship between the significantly low values of PI and the "second promontory" of the sacrum, demonstrating posterior convergence of the S1–S2 sacral plates in the SH sample, conforms to the modern sagittal anatomy. The particular relative position of S1 and S2 in the Neandertal lineage is the manifestation of one of the anatomical parameters related to the sagittal spino-pelvic balance.

Implications of the SH Pelvis 1 Individual Pathological Lesions. The sagittal anatomy of the lumbo-pelvic region is a main factor that determines the placement of the line of gravity and, therefore, the sagittal balance of the body over the hip joints. The SH Pelvis 1 individual was affected by lumbar kyphotic deformity and spondylolisthesis. Patients affected by these diseases may suffer from sagittal imbalance and postural disorders because of significant anterior displacement of their center of gravity (37, 39). Thus, patients can develop adaptive compensatory postural and muscular mechanisms (*SI Appendix*, Fig. S10*C*): pelvic backtilt [reduction of the SS, loss of LL, and increase of pelvic tilt (PT); that is, the angle between the vertical plane and the line running between the midpoints of the biacetabular axis and the sacral plate (36, 40)], development of a flat or lordotic curvature in the thoracic region (37), activation of the extensor hip muscles (e.g., gluteus maximus and hamstrings), and knee bending (25). All or part of these compensatory mechanisms are likely to have taken place in the SH Pelvis 1 individual, considering the number and severity of its lumbo-pelvic lesions. Nevertheless, because PI = SS ($\geq 0°$) + PT (40) and the PI value of Pelvis 1 is remarkable low, the capacity of this individual to back-tilt was much reduced.

Regardless of its balance and postural circumstances, modern patients suffering lumbar degenerative kyphosis show difficulties walking and carrying or lifting objects (36, 37), and Baastrup disease is associated with considerable lower back pain (41). In addition, several inflammatory processes were currently in progress at the moment of the SH pelvis 1 individual's death, as seen in the osteolytic lesion, the periosteal reactive bone and, likely associated with Baastrup disease, interspinous bursistis (41). These three signs are also patent manifestations of intense pain.

Baastrup disease has also been reported in Shanidar 2 and 3 and the La Chapelle-aux-Saints Neandertal individuals (23). This disease, together with other degenerative processes in the vertebral column of Neandertals, has been suggested to be related to high levels of strenuous physical activities and mechanical demands, such as habitual transport of heavy resources over extended distances (23). The hypolordotic lumbar column and the massive bodies of the SH population and Neandertals would also have resulted in high compressive forces in the spine, which is one of the pathognomonic conditions of the disc herniation and degeneration (28, 40). In summary, the distinct anatomy of the lumbo-pelvic region and lifestyle of *H. heidelbergensis* may have made them more susceptible to develop particular spinal and pelvic pathologies.

Conclusions

The advanced age-at-death (> 45 y) of the SH Pelvis 1 individual, coupled with signs of degenerative processes in the lumbar spine, can be interpreted as evidence of an aged individual, something that has been suggested previously for SH mandibles (42). Two important conclusions can be drawn from this theory. First, some of the *H. heidelbergensis* individuals from SH survived to relatively advanced ages. A trend of increasing older adult survivorship has been reported over the course of human evolutionary history based on the dental remains (43). Nevertheless, potential signs of senescence are occasionally preserved in cranial skeletal remains before the emergence of Neandertals (e.g., D3444/D3900) (44). Based on postcranial skeletal evidence, the SH Pelvis 1 individual represents the oldest evidence in the fossil record of an aged human. Second, this individual survived for a considerable period, with a suite of anomalies and pathological lesions. Some of these lesions would restrict, to a certain degree, the range of physical activities that they were able to perform. Comparison with present day hunter-gatherer societies suggests this individual would likely not have participated in hunting activities. However, this theory would not imply that it was no longer capable of moving with the social group. Survival of a second impaired individual from SH has also been

recently described (45). Thus despite the difficulties in demonstrating conspecific care based on fossil evidence (46), at least two individuals from the SH site survived for an undetermined (but probably considerable) period with serious cranial and postcranial impairments.

Materials and Methods

The SH Pelvis 1 individual is composed of 12 isolated bony elements coming from the SH site, consisting of the nearly complete five lumbar vertebrae (six fragments) and pelvis (six fragments) (Fig. 1, and *SI Appendix*, Text S1 and Table S1) These fragments were all found in a confined space of $1.0 \times 1.0 \times 0.2$ m^3 within the human-bearing clay deposits, affected by some in situ fractures, particularly the vertebrae, but not by plastic deformation (47) (*SI Appendix*, Fig. S11). Laboratory restoration was later undertaken to rejoin each of these fragments. Their subsequent association into a single individual was based on bilateral symmetry, developmental consistency, proper fitting along the joint surfaces, and pathological criteria (see above). The fossil and modern comparative samples are included in *SI Appendix*, Table S8. Several CT and surface scans were also performed (details in *SI Appendix*, Text S7).

The six bony elements comprising Pelvis 1 have been articulated by using high-resolution epoxy casts of each of these elements. The previous reconstruction was revised with the aim of minimizing the asymmetries about the sagittal plane (11), which has been done by placing the pubic symphysis along the sagittal plane of the pelvis. In brief, the isolated fragments composing Pelvis 1 have been articulated in the following sequence: (*i*) Articulation between the left and right ilium and ischium, and the sacrum. (*ii*) Reconstruction of the left pubic bone position by aligning the arcuate line and the ischio-pubic ramus, estimating the horizontal acetabular diameter and matching the pubic symphysis to the sagittal plane. (*iii*) Reconstruction of the position of both the right pubic body and the ischio-pubic ramus fragment by symmetry with the left side. The dorsal symphyseal demiface has been located as close as possible to the sagittal plane. Additional methodological aspects can be found in *SI Appendix, Texts* S3, S4, S6, and Fig. S6.

ACKNOWLEDGMENTS. We thank the Atapuerca excavation team, especially that of the Sima de los Huesos (A. Esquivel, R. Quam, N. García); M. C. Ortega and A. Citores for their work on the Pelvis 1 reconstruction; our colleagues at the Centro Mixto Universidad Complutense de Madrid–Instituto de Salud Carlos III de Evolución y Comportamiento Humanos (particularly to F. Gracia and J. Lira); the Laboratorio de Evolución Humana of Burgos University (especially to L. Rodríguez, R. García and E. Santos), and J. Trueba; and R. G. Franciscus, F. Gusi i Jener, Y. Haile-Selassie, P. Mennecier, M. Negro, R. Potts, J. Radovčić, Y. Rak, and the staff of the Instituto de Antropología of Coimbra University for access to the skeletal collections in their care. Technical assistance was provided by A. Fort, L. Huet, V. Laborde, L. Jellema, and J. Clark. We appreciate fruitful discussions with A. Bartsiokas, E. Been, R. Hernández, I. Hershkovitz, J. C. Ohman, A. Planillo, J. Rios, and the two reviewers. Help in the field from the Grupo Espeleológico Edelweiss was essential. This work was funded by the Ministerio de Ciencia e Innovación of Spain (CGL2006-13532-C03 and CGL2009-12703-C03), the Junta de Castilla y León (BU032A06 and BU005A09), and the SYNTHESYS Project (European Community Research Infrastructure Action, FP6 "Structuring the European Research Area" Programme). A.B. received a grant from the Fundación Atapuerca/Duques de Soria. Funding for the fieldwork came from the Junta de Castilla y León and Fundación Atapuerca.

1. Ohman JC, et al. (2002) Stature-At-Death of KNM-WT 15000. *Hum Evol* 17:129–142.
2. Endo B, Kimura T (1970) *The Amud Man and His Cave Site*, eds Suzuki H, Takai F (Academic Press, Tokyo), pp 231–406.
3. Trinkaus E (1976) The morphology of European and Southwest Asian Neandertal pubic bones. *Am J Phys Anthropol* 44:95–103.
4. Rak Y, Arensburg B (1987) Kebara 2 Neanderthal pelvis: First look at a complete inlet. *Am J Phys Anthropol* 73:227–231.
5. Weber J, Pusch CM (2008) The lumbar spine in Neanderthals shows natural kyphosis. *Eur Spine J* 17(Suppl 2):S327–S330.
6. Been E (2005) The anatomy of the lumbar spine of *Homo neanderthalensis* and its phylogenetic and functional implications. (Translated from Hebrew) PhD thesis (Tel Aviv University, Tel Aviv, Israel).
7. Been E, Peleg S, Marom A, Barash A (2010) Morphology and function of the lumbar spine of the Kebara 2 Neandertal. *Am J Phys Anthropol* 142:549–557.
8. Gómez-Olivencia A (2009) Paleobiological research on the vertebral column and thoracic cage of Pleistocene fossil humans, with special reference to the fossils from the Sierra de Atapuerca. (Translated from Spanish) PhD thesis (University of Burgos, Burgos, Spain).
9. McHenry HM (1975) A new pelvic fragment from Swartkrans and the relationship between the robust and gracile australopithecines. *Am J Phys Anthropol* 43:245–262.
10. Rosenberg K (1998) *Neandertals and Modern Human in Western Asia*, eds Akazawa T, Aoki K, Bar-Yosef O (Plenum, New York), pp 367–379.
11. Arsuaga JL, et al. (1999) A complete human pelvis from the Middle Pleistocene of Spain. *Nature* 399:255–258.
12. Simpson SW, et al. (2008) A female *Homo erectus* pelvis from Gona, Ethiopia. *Science* 322:1089–1092.
13. Arsuaga JL, Martínez I, Gracia A, Lorenzo C (1997) The Sima de los Huesos crania (Sierra de Atapuerca, Spain). A comparative study. *J Hum Evol* 33:219–281.
14. Martínez I, Arsuaga JL (1997) The temporal bones from Sima de los Huesos Middle Pleistocene site (Sierra de Atapuerca, Spain). A phylogenetic approach. *J Hum Evol* 33:283–318.
15. Bischoff JL, et al. (2007) High-resolution U-series dates from the Sima de los Huesos hominids yields 600 +infinite/–66 kyrs: Implications for the evolution of the early Neanderthal lineage. *J Archaeol Sci* 34:763–770.
16. Bermúdez de Castro JM, Martinón-Torres M, Lozano M, Sarmiento S, Muela A (2004) Paleodemography of the Atapuerca-Sima de los Huesos hominin sample: A revision and new approaches to the paleodemography of the European Middle Pleistocene population. *J Anthropol Res* 60:5–26.
17. Bonmatí A, Arsuaga JL (2005) Inventory and preliminary description of Middle Pleistocene pelvis remains from the site of Sima de los Huesos, Atapuerca (Spain). *Am J Phys Anthropol* 126(Suppl 40):76.
18. Ruff CB (2010) Body size and body shape in early hominins—Implications of the Gona pelvis. *J Hum Evol* 58:166–178.
19. Arsuaga JL, Martínez I, Gracia A (2001) Phylogenetic analysis of the hominids from Sierra de Atapuerca (Sima de los Huesos and Gran Dolina TD-6): The cranial evidence (Translated from French). *Anthropologie* 105:161–178.
20. Arsuaga JL, Carretero JM (1994) Multivariate analysis of the sexual dimorphism of the hip bone in a modern human population and in early hominids. *Am J Phys Anthropol* 93:241–257.
21. Weaver TD, Hublin JJ (2009) Neandertal birth canal shape and the evolution of human childbirth. *Proc Natl Acad Sci USA* 106:8151–8156.
22. Arensburg B (1991) *The Mousterian Skeleton of Kebara 2*, (Translated from French) eds Bar-Yosef O, Vandermeersch B (Éditions du CNRS, Paris), pp 113–147.
23. Ogilvie MD, Hilton CE, Ogilvie CD (1998) Lumbar anomalies in the Shanidar 3 Neandertal. *J Hum Evol* 35:597–610.
24. Digiovanni BF, Scoles PV, Latimer BM (1989) Anterior extension of the thoracic vertebral bodies in Scheuermann's kyphosis. An anatomic study. *Spine (Phila PA 1976)* 14:712–716.
25. Duval-Beaupère G, Schmidt C, Cosson P (1992) A barycentremetric study of the sagittal shape of spine and pelvis: The conditions required for an economic standing position. *Ann Biomed Eng* 20:451–462.
26. Peleg S, et al. (2007) Orientation of the human sacrum: Anthropological perspectives and methodological approaches. *Am J Phys Anthropol* 133:967–977.
27. Marty C, et al. (2002) The sagittal anatomy of the sacrum among young adults, infants, and spondylolisthesis patients. *Eur Spine J* 11:119–125.
28. Rajnics P, Templier A, Skalli W, Lavaste F, Illes T (2002) The importance of spinopelvic parameters in patients with lumbar disc lesions. *Int Orthop* 26:104–108.
29. Boulay C, et al. (2006) Sagittal alignment of spine and pelvis regulated by pelvic incidence: Standard values and prediction of lordosis. *Eur Spine J* 15:415–422.
30. Legaye J (2007) The femoro-sacral posterior angle: An anatomical sagittal pelvic parameter usable with dome-shaped sacrum. *Eur Spine J* 16:219–225.
31. Barnes E (1994) *Developmental Defects of the Axial Skeleton in Paleopathology* (University Press of Colorado, Niwot, Colorado).
32. Scheuer L, Black S (2000) *Developmental Juvenile Osteology* (Academic Press, London).
33. Pérez PJ (2003) *Paleopathology. The Unwritten Disease* (Translated from Spanish), eds Isidro A, Malgosa A (Masson, Barcelona), pp 295–306.
34. Ortner DJ (2003) *Identification of Pathological Conditions in Human Skeletal Remains* (Academic Press, New York).
35. Merbs CF (1996) Spondylolysis and spondylolisthesis: A cost of being an erect biped or a clever adaptation? *Am J Phys Anthropol* 39:201–228.
36. Takemitsu Y, Harada Y, Iwahara T, Miyamoto M, Miyatake Y (1988) Lumbar degenerative kyphosis. Clinical, radiological and epidemiological studies. *Spine (Phila PA 1976)* 13:1317–1326.
37. Jang JS, Lee SH, Min JH, Han KM (2007) Lumbar degenerative kyphosis: Radiologic analysis and classifications. *Spine (Phila PA 1976)* 32:2694–2699.
38. Baastrup CI (1933) On the spinous processes of the lumbar vertebrae and the soft tissues between them, and on pathological changes in that region. *Acta Radiol* 14:52–55.
39. Labelle H, et al. (2008) Spino-pelvic alignment after surgical correction for developmental spondylolisthesis. *Eur Spine J* 17:1170–1176.
40. Barrey C, Jund J, Noseda O, Roussouly P (2007) Sagittal balance of the pelvis-spine complex and lumbar degenerative diseases. A comparative study about 85 cases. *Eur Spine J* 16:1459–1467.
41. Clifford PD (2007) Baastrup disease. *Am J Orthop* 36:560–561.
42. Rosas A, Pérez PJ, Bone J (1999) Senescence in European Middle Pleistocene hominids: The Atapuerca evidence. *Hum Evol* 14:83–98.
43. Caspari R, Lee SH (2004) Older age becomes common late in human evolution. *Proc Natl Acad Sci USA* 101:10895–10900.
44. Lordkipanidze D, et al. (2005) Anthropology: The earliest toothless hominin skull. *Nature* 434:717–718.
45. Gracia A, et al. (2009) Craniosynostosis in the Middle Pleistocene human Cranium 14 from the Sima de los Huesos, Atapuerca, Spain. *Proc Natl Acad Sci USA* 106:6573–6578.
46. DeGusta D (2002) Comparative skeletal pathology and the case for conspecific care in Middle Pleistocene hominids. *J Archaeol Sci* 29:1435–1438.
47. Arsuaga JL, et al. (1997) Sima de los Huesos (Sierra de Atapuerca, Spain). The site. *J Hum Evol* 33:109–127.